

---

# Understanding Type II Supernovae

L. Zampieri<sup>1</sup>, M. Ramina<sup>1,2</sup> and A. Pastorello<sup>1,2</sup>

<sup>1</sup> INAF-Osservatorio Astronomico di Padova, Vicolo dell'Osservatorio 5, I-35122 Padova, Italy

<sup>2</sup> Dipartimento di Astronomia, Università di Padova, Vicolo dell'Osservatorio 2, I-35122 Padova, Italy

We present the results of a systematic analysis of a group of Type II plateau supernovae that span a large range in luminosities, from faint objects like SN 1997D and 1999br to very luminous events like SN 1992am. The physical properties of the supernovae appear to be related to the plateau luminosity or the expansion velocity. The simultaneous analysis of the observed light curves, line velocities and continuum temperatures leads us to robust estimates of the physical parameters of the ejected envelope. We find strong correlations among several parameters. The implications of these results regarding the nature of the progenitor, the central remnant and the Ni yield are also addressed.

## 1 Introduction

Type II supernovae (SNe) are believed to be core-collapse SNe originating from massive ( $> 8M_{\odot}$ ) red supergiants that retain their Hydrogen (H) envelopes. The overall phenomenological appearance of these SNe is rather well understood (see e.g. [1]). However, despite lightcurve and spectral modelling have provided important information on the physical properties of single objects (see e.g [7]), comparatively little effort has been devoted to study the correlations between the basic properties of Type II SNe and to understand to what extent the variety of their observational properties can be explained in terms of continuous changes of some fundamental physical variables. This is especially interesting after the recent discovery of a group of low luminosity (LL),  $^{56}\text{Ni}$  poor SNe [5, 8], whose relation with the “normal” and more luminous Type II events is still under debate. The work in this area has certainly been hampered also by the very heterogeneous behavior of Type II SNe. However, a recent investigation has shown that significant correlations exist among the plateau luminosity, the expansion velocity measured at 50 days after the explosion and the ejected  $^{56}\text{Ni}$  mass [2]. Here we present the results of a systematic analysis of a group of Type II plateau supernovae that extends, especially at very low luminosity, the sample previously considered. While

we confirm the results of Hamuy [2], we do not find evidence of a definite correlation between the ejected envelope mass and the other parameters.

## 2 Selected Sample of Type II Plateau SNe

The data were taken from literature and/or extracted from the large database of lightcurves and spectra of the Padova-Asiago Supernova Archive. A description of the selection process is outlined in Pastorello et al. (these Proceedings). Observations of SN 2003Z<sup>3</sup>, the first LL event extensively monitored from explosion up to the nebular stage, are also included in this work. SNe with uncertain estimates of the distance and interstellar absorption and/or with signs of significant interaction with the circumstellar material were not considered. The main selection criterion was to choose objects that cover a big range in luminosity, including LL, 97D-like events [5, 8] and luminous 92am-like objects [6]. The selected objects are reported in Table 1. Most of them have a good photometric coverage until 300–400 days after the explosion and at least 4–5 spectra in the photospheric phase (up to  $\sim 100 - 120$  days). The best available estimates of the explosion epoch, the distance modulus and interstellar absorption (Galactic and internal) for these objects are reported in Pastorello et al. (these Proceedings) and Ramina (Laurea Thesis, unpublished). SN 1987A is included for comparison.

## 3 Modelling Core-collapse SNe

In the present analysis the physical parameters of the selected sample of SNe are derived comparing the observational data to model calculations. The adopted model is a semi-analytic code that solves the energy balance equation for a spherically symmetric, homologously expanding envelope at constant density [8]. The initial conditions are rather idealized and provide an approximate description of the ejected material after shock (and possible reverse shock) passage, as derived from hydrodynamical calculations. In particular, elements are assumed to be completely mixed throughout the envelope and their distribution depends only on the coordinate mass. Hydrogen, Helium, Carbon and Oxygen are assumed to be uniformly distributed, whereas <sup>56</sup>Ni is more centrally peaked. The evolution of the expanding envelope is computed including all the relevant energy sources powering the SN and is schematically divided in 3 phases from the photospheric up to the late nebular stages (for more details see Zampieri et al. [8] and Ramina [Laurea Thesis, unpublished]). The most important quantities computed by the code are the light curve and the evolution of the line velocity and continuum temperature at the photosphere. The physical properties of the envelope are derived by performing a simultaneous fit of these three observables with model calculations.

<sup>3</sup> Made in part at the Telescopio Nazionale Galileo (TNG) under program TAC\_48.

## 4 Correlations Among Physical Parameters

The physical parameters of the post-shock, ejected envelope are listed in Table 1. Only some of them are input parameters ( $R_0$ ,  $M_{env}$ ,  $V_0$ ,  $T_{eff}$ ), while the others are computed by the code or fixed by the observations. Two other input physical constants are the fraction of the initial energy that goes into kinetic energy  $f_0$  and the gas opacity  $\kappa$ . In this calculation we adopt  $f_0 = 0.5$  (initial equipartition between thermal and kinetic energies) and  $\kappa = 0.2 \text{ cm}^2 \text{ g}^{-1}$  (appropriate for an envelope comprised of He and iron-group elements). The color correction factor  $f_c = T_c/T_{eff}$ , that measures the deviation of the continuum radiation temperature  $T_c$  from the blackbody effective temperature  $T_{eff}$ , was kept fixed and equal to 1.2.

**Table 1.** Physical parameters from the semi-analytic model

	$R_0$ ( $10^{12} \text{ cm}$ )	$M_{env}$ ( $M_\odot$ )	$M_{Ni}$ ( $M_\odot$ )	$V_0$ ( $10^8 \text{ cm s}^{-1}$ )	$E$ ( $10^{51} \text{ erg}$ )	$t_{rec,0}$ (days)	$T_{eff}$ (K)	$\log L_p$
1992am	41 <sup>+6</sup> <sub>-5</sub>	26 <sup>+8</sup> <sub>-3</sub>	0.41 <sup>+0.04</sup> <sub>-0.04</sub>	5.1 <sup>+0.5</sup> <sub>-0.4</sub>	8.1 <sup>+4.1</sup> <sub>-2.0</sub>	53	4400 <sup>+400</sup> <sub>-300</sub>	42.55
1992H	38 <sup>+3</sup> <sub>-2</sub>	23 <sup>+7</sup> <sub>-3</sub>	0.18 <sup>+0.01</sup> <sub>-0.01</sub>	4.9 <sup>+0.2</sup> <sub>-0.4</sub>	6.6 <sup>+2.7</sup> <sub>-1.8</sub>	50	4300 <sup>+200</sup> <sub>-200</sub>	42.4
1996W	37 <sup>+5</sup> <sub>-3</sub>	16 <sup>+4</sup> <sub>-2</sub>	0.17 <sup>+0.02</sup> <sub>-0.02</sub>	4.1 <sup>+0.3</sup> <sub>-0.3</sub>	3.2 <sup>+1.3</sup> <sub>-0.8</sub>	48	4500 <sup>+400</sup> <sub>-300</sub>	42.25
1995ad	17 <sup>+3</sup> <sub>-2</sub>	12 <sup>+2</sup> <sub>-2</sub>	0.029 <sup>+0.003</sup> <sub>-0.004</sub>	4.0 <sup>+0.4</sup> <sub>-0.4</sub>	2.3 <sup>+0.9</sup> <sub>-0.7</sub>	30	4700 <sup>+300</sup> <sub>-200</sub>	41.9
1969L	25 <sup>+3</sup> <sub>-2</sub>	16 <sup>+2</sup> <sub>-1</sub>	0.067 <sup>+0.006</sup> <sub>-0.005</sub>	3.6 <sup>+0.2</sup> <sub>-0.2</sub>	2.5 <sup>+0.6</sup> <sub>-0.4</sub>	50	4300 <sup>+200</sup> <sub>-10</sub>	42.0
1987A	6 <sup>+0.9</sup> <sub>-0.7</sub>	18 <sup>+4</sup> <sub>-2</sub>	0.075 <sup>+0.006</sup> <sub>-0.006</sub>	2.8 <sup>+0.2</sup> <sub>-0.2</sub>	1.7 <sup>+0.6</sup> <sub>-0.4</sub>	26	4300 <sup>+100</sup> <sub>-200</sub>	41.35
1996an	19 <sup>+2</sup> <sub>-3</sub>	13 <sup>+2</sup> <sub>-1</sub>	0.050 <sup>+0.005</sup> <sub>-0.005</sub>	3.3 <sup>+0.1</sup> <sub>-0.2</sub>	1.7 <sup>+0.3</sup> <sub>-0.3</sub>	46	4200 <sup>+200</sup> <sub>-100</sub>	41.8
1999em	14 <sup>+3</sup> <sub>-2</sub>	14 <sup>+2</sup> <sub>-1</sub>	0.022 <sup>+0.002</sup> <sub>-0.003</sub>	3.2 <sup>+0.1</sup> <sub>-0.2</sub>	1.7 <sup>+0.4</sup> <sub>-0.3</sub>	48	3800 <sup>+100</sup> <sub>-200</sub>	41.6
1992ba	13 <sup>+2</sup> <sub>-1</sub>	17 <sup>+2</sup> <sub>-2</sub>	0.016 <sup>+0.003</sup> <sub>-0.002</sub>	3.2 <sup>+0.2</sup> <sub>-0.4</sub>	2.1 <sup>+0.5</sup> <sub>-0.7</sub>	42	3500 <sup>+200</sup> <sub>-300</sub>	41.5
2003Z	13 <sup>+2</sup> <sub>-1</sub>	19 <sup>+2</sup> <sub>-2</sub>	0.006 <sup>+0.001</sup> <sub>-0.002</sub>	2.2 <sup>+0.2</sup> <sub>-0.1</sub>	1.1 <sup>+0.3</sup> <sub>-0.2</sub>	28	4000 <sup>+200</sup> <sub>-200</sub>	41.25
1997D	10 <sup>+0.5</sup> <sub>-0.5</sub>	17 <sup>+3</sup> <sub>-2</sub>	0.008 <sup>+0.001</sup> <sub>-0.002</sub>	2.1 <sup>+0.2</sup> <sub>-0.2</sub>	0.9 <sup>+0.3</sup> <sub>-0.2</sub>	32	3900 <sup>+200</sup> <sub>-200</sub>	41.15
1994N	16 <sup>+1</sup> <sub>-3</sub>	15 <sup>+2</sup> <sub>-2</sub>	0.0068 <sup>+0.0003</sup> <sub>-0.0003</sub>	2.1 <sup>+0.2</sup> <sub>-0.2</sub>	0.8 <sup>+0.3</sup> <sub>-0.2</sub>	38	4200 <sup>+300</sup> <sub>-200</sub>	41.4
2001dc	10 <sup>+1</sup> <sub>-1</sub>	12 <sup>+2</sup> <sub>-2</sub>	0.0058 <sup>+0.0005</sup> <sub>-0.0007</sub>	1.9 <sup>+0.3</sup> <sub>-0.2</sub>	0.5 <sup>+0.3</sup> <sub>-0.1</sub>	27	4000 <sup>+200</sup> <sub>-200</sub>	41.1
1999eu	8 <sup>+0.4</sup> <sub>-0.6</sub>	12 <sup>+2</sup> <sub>-1</sub>	0.003 <sup>+0.0005</sup> <sub>-0.0004</sub>	1.8 <sup>+0.3</sup> <sub>-0.1</sub>	0.5 <sup>+0.3</sup> <sub>-0.1</sub>	38	3600 <sup>+200</sup> <sub>-100</sub>	40.9
1999br	7 <sup>+0.4</sup> <sub>-0.6</sub>	15 <sup>+2</sup> <sub>-2</sub>	0.0021 <sup>+0.0002</sup> <sub>-0.0002</sub>	1.8 <sup>+0.1</sup> <sub>-0.2</sub>	0.6 <sup>+0.1</sup> <sub>-0.2</sub>	33	3400 <sup>+100</sup> <sub>-200</sub>	40.85

$R_0$  is the initial radius of the ejected envelope at the onset of expansion

$M_{env}$  is the ejected envelope mass

$M_{Ni}$  is the ejected  $^{56}\text{Ni}$  mass

$V_0$  is the velocity of the homologously expanding envelope at the outer shell

$E$  is the initial thermal+kinetic energy of the ejected envelope

$t_{rec,0}$  is the time when the envelope starts to recombine

$T_{eff}$  is the effective temperature during recombination

$L_p$  Luminosity (BVRI bands) at  $t_{rec,0}$  (plateau luminosity)

As shown in Figure 1 (left panel), the inferred physical parameters of the ejected envelope are strongly correlated. All quantities appear to vary continuously with the plateau luminosity  $L_p$  or, alternatively, with the expansion

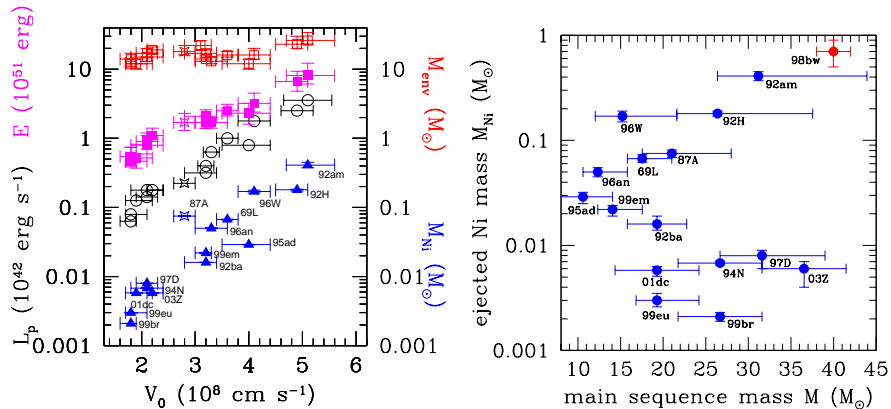


**Fig. 1.** *Left:* Luminosity  $L_p$  (circles), energy  $E$  (filled squares), envelope mass  $M_{env}$  (open squares) and  $^{56}\text{Ni}$  mass  $M_{Ni}$  (triangles) vs expansion velocity  $V_0$  for the SNe of our sample. The asterisks denote SN 1987A. *Right:* Ejected  $^{56}\text{Ni}$  mass  $M_{Ni}$  vs inferred progenitor main sequence mass  $M$ . SN 1998bw is shown for comparison.

velocity of the envelope at the outer shell  $V_0$ , which coincides with the photospheric velocity measured at the onset of recombination. In particular, the  $^{56}\text{Ni}$  mass increases with  $V_0$  over several orders of magnitude. The sole exception is the ejected envelope mass  $M_{env}$  that, within the estimated errors, does not show any definite tendency to vary with the other parameters. Only at high velocities (and luminosities) does  $M_{env}$  increase slightly with  $V_0$ .

Correlations between the observed luminosity and photospheric velocity at 50 days after the explosion, and between the observed luminosity and inferred ejected  $^{56}\text{Ni}$  mass have recently been reported by Hamuy [2]. Our results confirm his findings and clarify that the physical variable associated to the photospheric velocity at 50 days after the explosion is the expansion velocity  $V_0$ . It is worth noting also that LL, Ni-poor SNe, such as SN 1997D and SN 1999br, do not appear to occupy a separate area of the diagram but, instead, populate the low energy tail of the correlation, showing a continuum variation of their parameters with respect to their more energetic cousins.

The very weak dependence of  $M_{env}$  on the other parameters has important consequences for the nature of the progenitor and the compact remnant. We derived a rough estimate of the progenitor main sequence mass  $M$  assuming no mass loss and a simple but physically plausible “mixing recipe”, that is the fraction of Carbon-Oxygen-Helium mass  $M_{mix}$  mixed into the hydrogen layer and ejected increases with increasing  $^{56}\text{Ni}$  yield or expansion velocity ( $f_{mix} = M_{mix}/M_{env} = 0.15$  for the LL events,  $f_{mix} = 0.4$  for the “normal” Type II SNe,  $f_{mix} = 0.45$  for the high luminosity objects). The results are not strongly dependent on the specific prescription for mixing, as long as it is taken to increase with  $M_{Ni}$  or  $V_0$ . From this, assuming no rotation, we then estimate

the hydrogen mass from  $M_H = M_{env} - M_{mix} = (1 - f_{mix})M_{env}$  and the main sequence mass from the approximate expression  $M = 2.9(1 - f_{mix})M_{env} - 10.3$  (see e.g. [1]). Including mass loss would result in larger values of  $M$ , especially for  $M \geq 20M_\odot$ , with a significant dependence on metallicity. We find that both high and LL SNe have massive progenitors with  $M \geq 20 - 25M_\odot$ . This follows, for the first, from the large inferred value of  $M_{env}$  while, for the second, from the fact that  $f_{mix}$  is small. Because “normal” and LL events have similar ejected envelope masses  $M_{env}$  but rather different mixing fractions, the first have comparatively less massive progenitors ( $12 \leq M \leq 20M_\odot$ ). For the “normal” and high luminosity SNe a large fraction of the ejected envelope mass comes from the Carbon-Oxygen-Helium layer that was successfully ejected, while in the LL events  $M_{env}$  essentially measures the ejected Hydrogen mass. Despite the large errors, we find that only LL SNe appear to have progenitors with masses significantly in excess of  $M_{env}$ . Thus, they may have undergone significant fallback, as suggested by Zampieri et al. [8], and harbor rather massive black holes.

In Figure 1 (right panel) we show the plot of the ejected  $^{56}\text{Ni}$  mass versus the inferred progenitor main sequence mass. Again, albeit the errors are very large, it is possible to recognize that Type II SNe populate different regions in this diagram. In particular, as originally suggested by Iwamoto et al. [3], there appears to be a bimodal behavior above  $\approx 20M_\odot$ , with high luminosity events populating the high  $^{56}\text{Ni}$  tail (close to the area occupied by hypernovae as SN 1998bw) and LL objects filling the low  $^{56}\text{Ni}$  yield region. The reason for the large spread in ejected  $^{56}\text{Ni}$  and the non monotonic behavior of the  $M - M_{Ni}$  relation is not clear. Perhaps, as suggested by Maeda and Nomoto [4], in luminous events a large amount of angular momentum is retained by the post-shock envelope causing the formation of jets and an enhanced energy release along the jet axes, whereas “normal” and LL events may have more spherical shapes. It could also be that different metallicities and mass loss histories prior to explosion play an important role, with high luminosity events having more powerful winds while LL ones retain almost all their hydrogen envelope until explosion.

## References

1. W.D. Arnett: *Supernovae and Nucleosynthesis* (Princeton University Press, Princeton 1996)
2. M. Hamuy: ApJ **582**, 905 (2003)
3. K. Iwamoto, T. Nakamura, K. Nomoto et al: ApJ **534**, 660 (2000)
4. K. Maeda, K. Nomoto: ApJ (2003), in press
5. A. Pastorello, L. Zampieri, M. Turatto et al: MNRAS (2003), in press
6. B. Schmidt, R.P. Kirshner, R.G. Eastman et al: AJ **107**, 1444 (1994)
7. S.E. Woosley: ApJ **330**, 218 (1988)
8. L. Zampieri, A. Pastorello, M. Turatto et al.: MNRAS **338**, 711 (2003)